

Reconstructing seasonality using $\delta^{18}\text{O}$ in incremental layers of human enamel: a test of the analytical protocol developed for *SHRIMP IIe/MC* ion microprobe

Ewa KRZEMIŃSKA¹*, Arkadiusz SOŁTYSIAK² and Zbigniew CZUPYT¹

¹ Polish Geological Institute – National Research Institute, Rakowiecka 4, 00-975 Warszawa, Poland

² University of Warsaw, Institute of Archaeology, Department of Bioarchaeology, Krakowskie Przedmieście 26/28, 00-927 Warszawa, Poland

Krzemińska, E., Sołtysiak, A., Czupyt, Z., 2017. Reconstructing seasonality using $\delta^{18}\text{O}$ in incremental layers of human enamel: a test of the analytical protocol developed for *SHRIMP IIe/MC* ion microprobe. *Geological Quarterly*, **61** (2): 370–383, doi: 10.7306/gq.1354



A number of recent studies dealing with palaeoclimate and environmental reconstruction include the measurement of oxygen isotope composition of mammalian teeth. Some of them analyse a temporal sequence of the changes recorded in bioapatite from enamel layers representing the whole period of tooth development. Enamel samples display large intra-tooth $\delta^{18}\text{O}$ variations that may reflect a seasonal fluctuation in the $\delta^{18}\text{O}$ of local palaeoclimate parameters. The present paper provides an effective analytical protocol for sequential $\delta^{18}\text{O}$ analysis of human teeth using *SHRIMP IIe/MC* ion microprobe. It is possible to follow the inner enamel layer along enamel-dentine junction on a high spatial scale in a range about 0.02 mm of spot diameter and 0.12–0.14 mm of the distance between spots. Using the methodology described herein, we can achieve an external precision for $\delta^{18}\text{O}$ analysis $<0.2\text{‰}$ (1σ). The number of 60 to 90 single analyses covering the enamel layer between the incisal and apical ends is enough to obtain temporal resolution of less than one month and to document precisely seasonal fluctuation caused by local environmental and climate factors. The methodology of $\delta^{18}\text{O}$ *in situ* measurements has been tested on human teeth from Tell Majnuna, a 4th millennium BCE cemetery in Northern Mesopotamia, which is a relatively arid area with high seasonal differences in precipitation and temperature. Observed pattern of $\delta^{18}\text{O}$ variations is consistent with expected seasonal fluctuations, although the overall effect is blurred by some inertia in the enamel maturation.

Key words: palaeoclimate, bioapatite, human teeth, sequential microsampling, Middle East, Mesopotamia.

INTRODUCTION

Oxygen isotope analysis of dental enamel is a powerful tool for palaeobiological and archaeological studies as an indicator of the parameters of physiology, natural environment and habitat preferences. A particularly promising approach is to measure intra-tooth variation (Ballase, 2003; Blaise and Balasse, 2011; Stevens et al., 2011), because teeth accumulate a sequence of significant isotopic information covering the short time of enamel bioapatite progressive formation.

The oxygen isotope investigations of mammalian dental enamel are based on a few general assumptions that:

- the tissues of organism isotopically equilibrated with their environment will reflect the local environmental oxygen ratio;
- isotopic signature of skeletal tissues is directly related to that of the local drinking water;

- bioapatite, the main component of teeth, is relatively most resistant to diagenetic processes and preserves its biogenic isotopic signature.

Under a constant temperature of 37°C of mammalian body, the oxygen isotope ratio within dental enamel essentially depends on the oxygen isotope composition of water ingested by the organism. Between the water and bioapatite, oxygen isotope is fractionated in two steps, i.e. between environmental and body water and between body water and bioapatite in teeth and bones (Bryant and Froelich, 1995). Moreover, the oxygen isotope composition of enamel remains fixed (i.e. enamel is no longer metabolized by the body), providing a nearly continuous stable isotope record that may cover a period from months to years and that can be retained for thousands of years after fossilization (Kohn and Cerling, 2002).

The isotopic analysis of enamel has been used to study seasonal dietary habits of both modern and archaeological fauna (Fricke and O'Neil, 1996; Stuart-Williams and Schwarcz, 1997; Fricke et al., 1998; Balasse, 2003; Blaise and Balasse, 2011; Stevens et al., 2011), however, sequential intra-tooth isotopic variation has received little attention in the studies of archaeological human remains.

The oxygen isotopic composition of human bioapatite is related to the isotopic composition of local drinking water (Longinelli, 1984; Luz et al., 1984). In most locations, availability of po-

* Corresponding author, e-mail: ewa.krzeminska@pgi.gov.pl

Received: October 10, 2016; accepted: December 20, 2016; first published online: March 24, 2016

table water depends mainly on the rainfall (Babu et al., 2011). During prehistorical and historical times, drinking water was taken mainly from surface sources. Therefore, the oxygen isotopic record from ancient samples predominantly reflects local precipitation, although in some locations the use of wells may make this relation less straightforward.

Human teeth record isotopic information during the period of enamel growth. It depends on the local environment, including water precipitation, amount of rainfall (or atmospheric humidity), the distance from the coast, ambient temperature, latitude and altitude, as well as diet and migration events (Fricke and O'Neil, 1996; Gregoricka, 2011). Positive correlation between isotopic composition of enamel and past meteoritic water is extensively used to deduce climate anomalies of mean annual air temperatures (Pflug et al., 1979; Luz and Kolodny, 1985; Fricke et al., 1995, 1998; Amiot et al., 2006; Aubert et al., 2012; Blumenthal et al., 2014). Sub-annual time series of isotopic variation of environmental water composition are encoded as an isotopic zoning across incremental enamel layers. Serial sampling in microscale (microsampling) to extract these variations has become a basic methodology (Trayler and Kohn, 2017) to investigate seasonal fluctuations of climate factors.

The process of measurements of oxygen isotope composition expressed as $^{18}\text{O}/^{16}\text{O}$ ratios ($\delta^{18}\text{O}$) is typically conducted by conventional gas isotope-ratio mass-spectrometry IRMS technique. This methodology, however, is complex and destructive. About 20 micrograms of enamel bioapatite must be chemically purified from other oxygen sources in the enamel mineral matrix, mainly hydroxyl and carbonate ions, and trace quantities of organics. Then, chemical oxidation of bioapatite by sodium hypochlorite leads to removal of residual organic constituents after reaction of silver phosphate (Ag_3PO_4) with precise proportions of graphite to form CO_2 (O'Neil et al., 1994; Lécuyer et al., 1998). Both the phosphate and carbonate components of bioapatite are available for analysis. Some parts of studies have primarily utilized the phosphate because the P-O bond of the PO_4 molecule is stronger than the C-O and more diagenetically resistant (Sponheimer and Lee-Thorp, 1999), but oxygen extraction from the carbonate molecule is a much more easy procedure (Iacumin et al., 1996; Sponheimer and Lee-Thorp, 1999), thus, for such reason, is also commonly used.

The measurements of $\delta^{18}\text{O}$ in enamel micro-incremental growth layers, which may preserve a seasonal changes (Kohn et al., 1998), require a technique that provides an access to discrete regions of interest within those materials, and which allows minimizing destruction of irreplaceable materials of archaeological samples (Dolphin et al., 2016). These requirements can be filled by application of three secondary ion mass spectrometry (SIMS) technique on ion microprobe. In comparison to conventional IRMS, a SIMS does not include chemical preparation and sample homogenization. Furthermore, it enables *in situ* analyses on sub-nanogram domains within the polished surface of a target on spots sized in the range of 10–20 μm and 2–3 μm depth, reaching analytical precision similar to gas source IRMS. Thus, SIMS is an alternative tool for microscale sampling of dental bioapatite within incremental zones that are too narrow for conventional microdrilling. SIMS represents *in situ* measurements that provide a bulk analysis. In case of bioapatite, it includes all oxygen components, including OH and CO_3 . In another words, the $\delta^{18}\text{O}$ isotope signature observed on SIMS will be that of the oxygen present at three sites in apatite (CO_3^{2-} , PO_4^{3-} , H_2O), providing a more complete and realistic documentation of isotopic composition than conventional IRMS analyses (Wheeley et al., 2012; Williams et al., 2013).

SIMS technique for $\delta^{18}\text{O}$ analysis of bioapatite has been successfully applied on single conodonts during the last few years (Trotter et al., 2008, 2015; Wheeley et al., 2012), yielding temperatures of the palaeo-sea surface at critical periods of biotic crisis and environmental change in Paleozoic and Early Mesozoic time. There are only a few examples of $\delta^{18}\text{O}$ bioapatite measurements on mammalian dental tissues, which only demonstrate the potential of SIMS to provide *in situ* precise analysis of the oxygen isotopic compositions of biogenic materials with a spatial resolution of a few microns (Aubert et al., 2012; Blumenthal et al., 2014; Krzemińska and Czupyt, 2015). These authors explored the feasibility of SIMS microanalysis in tooth enamel of modern rodents (Blumenthal et al., 2014), fossil herbivores (deer and bison) and a Neandertal from Payre, France (Aubert et al., 2012), as well as a reindeer and bear dental enamel from Stajnia Cave (Żarski et al., 2017), confirming the significant usefulness of this technique to palaeoecological studies.

The exploration of oxygen isotope variation within human enamel is more difficult to interpret due to complexity of cultural behaviour, e.g. unpredictable water sources, more complex diet, and migration, which can provide an additional variable *versus* constant factors into the isotopic results. Therefore, the technique that offers a high spatial resolution of microsampling with sensitive detection of isotope composition within inner layers of enamel can effectively support the interpretation of $\delta^{18}\text{O}$ variability.

The aims of this study were to prepare and then to test the optimal analytical procedure for oxygen stable isotope *in situ* measurements within the innermost enamel layer by SHRIMP *Ile/MC* (enhanced Sensitive High Resolution Ion MicroProbe with multicollector), and to decipher the $\delta^{18}\text{O}$ isotopic record within human tooth enamel, and finally to evaluate the effects of intra-tooth variability in $\delta^{18}\text{O}$ ratios for palaeoclimate studies.

Human teeth were sampled from Tell Majnuna in North Mesopotamia (Fig. 1), near Tell Brak that represented one of the most significant ancient sites in the region, with recorded occupation from the 7th to 2nd millennia BCE. The area of present-day northeastern Syria is characterized by long hot and dry summers and relatively cool and humid winters with short transition seasons between. In case of specific locations where the annual amplitude of humidity and temperature is high, we can expect that changes in $\delta^{18}\text{O}$ values should fit to the summer/winter seasonal variation pattern. We checked whether any effect of high annual amplitude of humidity or/and temperature may be observed in teeth of two individuals from Tell Majnuna, buried at the cemetery dated to the 4th millennium BCE.

HUMAN ENAMEL AS THE POTENTIAL SOURCE OF INFORMATION ABOUT PAST CLIMATIC VARIABILITY

Enamel is the hardest tissue of a human organism and it includes only <1% of organic matter (Robinson et al., 1971; Nanci, 2013). Once formed, enamel does not remodel and is relatively stable, only with possible ion exchange and mechanical wear affecting exposed surfaces. The deeper part of enamel is well-isolated from the environment and its chemical composition is almost exclusively determined by the processes of enamel secretion and maturation during fetal growth, infancy and childhood (Nanci, 2013). The dominant mineral component of tooth enamel is biogenic apatite, i.e. a crystalline form of cal-

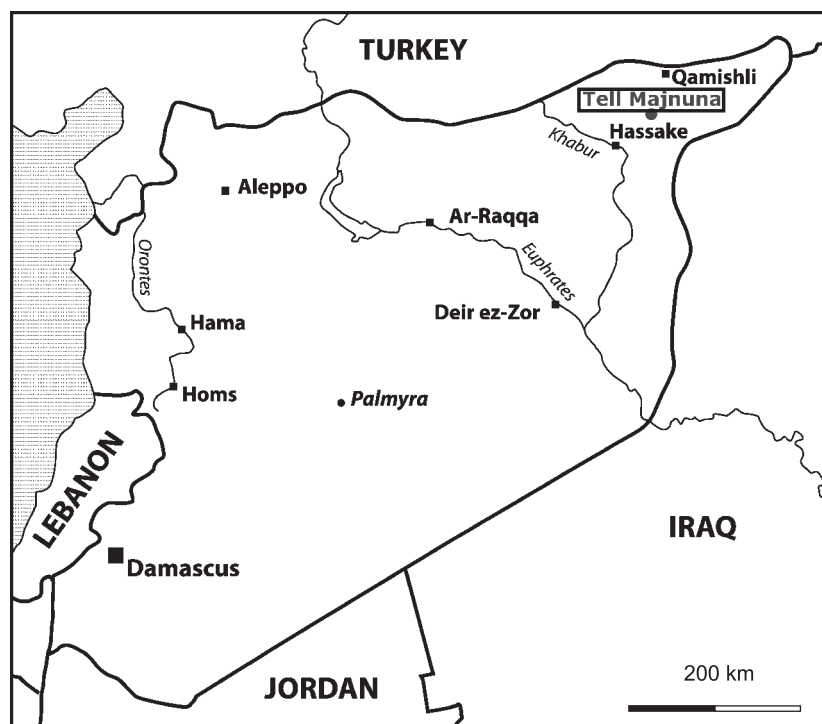


Fig. 1. Map of Syria showing the location of Tell Majnuna

cium phosphate (Eanes, 1979). Apatite is expressed by the general formula $\text{Ca}_{10}(\text{PO}_4)_6\text{X}_2$, where X may be represented by either F, Cl or OH, or a combination of these. Therefore members of mineral apatite-group are remarkably diverse in their major and trace element compositions because numerous substitutions that can occur without substantial changing of the basic lattice structure (e.g., Pan and Fleet, 2002). Biogenic apatites generally have a calcium hydroxyl-fluorapatite framework with common substitutions of Sr^{2+} replacing Ca^{2+} and CO_3^{2-} occupying PO_4^{3-} and OH^- positions (LeGeros et al., 1969; Eanes, 1979; Sønju Clasen and Ruyter, 1997). Natural porosity of bioapatite, that provides the pore space for diagenetic fluids, decreases from ~40 to ~1% from bone to dentine to enamel. Moreover, enamel is composed of tightly packed crystallites of bioapatite, which are ~50–100 nm in diameter (Hillson, 1996; Enax et al., 2012), and has a lower water and organic matter content in contrast to dentine (Fig. 2). In consequence, dental enamel is practically inert to isotopic exchange with water in low-temperature inorganic chemical systems and more resistant to alteration compared to dentine or bone (Lee-Thorp and van der Merwe, 1991; Ayliffe et al., 1994; Shahack-Gross et al., 1999).

The process of enamel formation may be generally divided into three stages:

- secretion of an organic matrix by ameloblasts;
- early formation of mineral crystals and removal of the organic matrix;
- enamel maturation.

In the early stage, the organic matrix promotes the development of octacalcium phosphate crystals that are subsequently hydrolyzed to final hydroxyapatite. At one time, the whole plane of enamel prisms measuring 3–8 μm (Fig. 2) is being formed, and when they are initially mineralized after a few days, the layer of new enamel enters into the maturation phase and the ameloblasts start forming a new layer (Simmer and Fincham,

1995). At the end of the initial phase of enamel formation, about 30% of mineral mass is already embedded into the enamel prism. The maturation phase is much longer and the formation of enamel may last for several years, even after eruption of a tooth. However, the intensity of this process decreases with time, and therefore it is possible to assume that most of the hydroxyapatite in a single prism is already mineralized during several weeks after the end of the initial formation phase (Nanci, 2013). The process of enamel formation in permanent teeth continues for 4–5 years from the top of the crown down to the cemento-enamel junction. After complete mineralisation, single enamel layers may be still recognized, as they are divided by striae of Retzius extending from the junction of enamel and dentin to the surface of the enamel (Fig. 3). Spaces between successive striae represent 6–11 days of initial enamel formation (Nanci, 2013).

The chemical composition of every enamel layer is determined not only during a few days of initial formation, but also during an unknown period of maturation, yet the set of high resolution $\delta^{18}\text{O}$ measurements in single (or neighbouring) layers retains the correct chronological pattern during the period of enamel formation and maturation. On the basis previous studies (Tafforeau et al., 2007; Blumenthal et al., 2014), the aprismatic innermost bulk of enamel is recommended for isotopic analyses. This zone of dental enamel extending <20 μm from the enamel-dentine junction was mineralized early in enamel maturation, and therefore may preserve an unchanged biogenic oxygen isotope signal that is less attenuated than in other layers, and more closely follows the chronology of incremental features.

The oxygen isotope signature of mammalian bioapatite, including tooth enamel, is determined by many variables that control oxygen fractionation. A species-specific diet (e.g., consumption of solid food, particularly vegetables), physiological effects, and the environment may influence the oxygen isotope

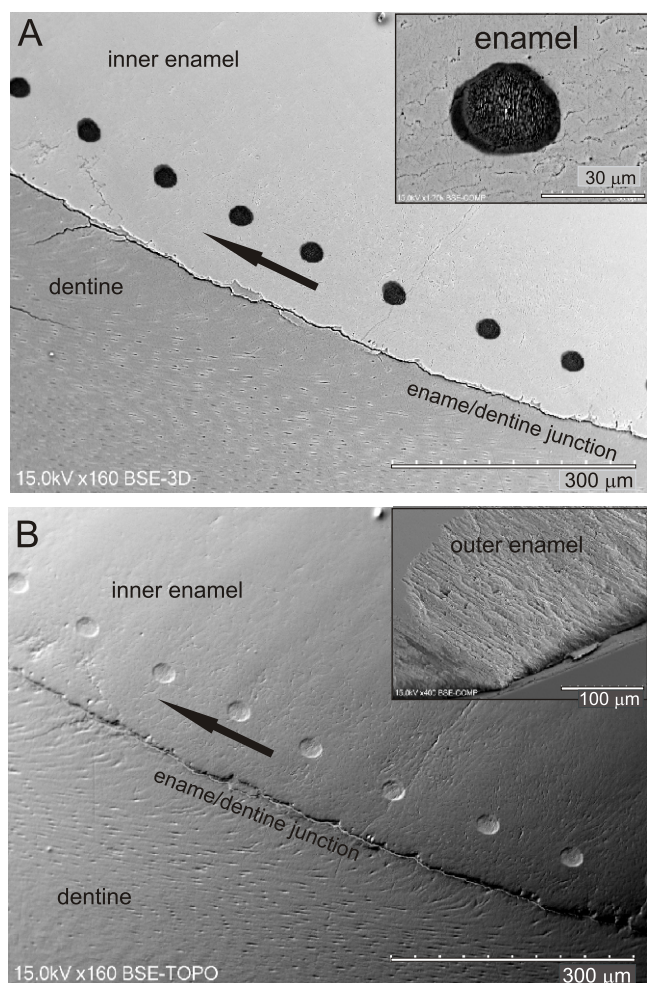


Fig. 2. Scanning electron micrograph of human teeth enamel

A – backscattered BSE image of analytical spot location close to enamel dentine junction, and size of sputtered spot by primary ion beam (insert). **B** – combined BSE and topographic image of tooth surface showing dentine/enamel junction, different porosity and hardness of dentine part, and shallow craters after isotopic measurement. Closer view of prism structure of bioapatite from outer part of enamel. The arrows indicate main direction of sequential analyses and maturation

enrichment between ingested water and enamel. Despite the combined effects of these factors on the isotopic composition of mammalian teeth (Table 1), the oxygen isotope composition of human bioapatite mainly reflects the $\delta^{18}\text{O}$ value of local source water (Longinelli, 1984; Luz et al., 1984; Luz and Kolodny, 1985; Dupras and Schwarcz, 2001). The $\delta^{18}\text{O}$ water value varies seasonally due to a range of climatic variables including the amount of precipitation and air temperature at middle to high latitudes; it tends to be more positive in summer (e.g., Rózański et al., 1993; Gregoricka, 2011).

Research on stable oxygen isotopes has been adopted to bioarchaeology from geology more than 20 year ago (e.g., Schoeninger, 1995; White et al., 1998). However, while geologists use $\delta^{18}\text{O}$ values mainly to trace for climatic changes in the past, in research on archaeological human remains this method was applied to search for past migrations between zones of different altitude, precipitation and/or sources of water (Lightfoot and O'Connell, 2016; Pellegrini et al., 2016; Tomczyk et al., 2016), or to estimate the timing of the weaning process (Jay, 2009; Tsutaya and Yoneda, 2015; Britton et al., 2015). The is-

sue of short-term weather and climatic fluctuations affecting $\delta^{18}\text{O}$ values in human tissues was so far rather neglected in bioarchaeological literature.

STUDY AREA: THE MARGINAL DRY FARMING ZONE OF NORTH MESOPOTAMIA

Tell Majnuna, a satellite site near Tell Brak, lies at the southern edge of the Upper Khabur drainage system that feeds the Euphrates River in Northern Mesopotamia. The Khabur drainage in the northeastern part of Syria is characterized by semi-arid steppe climate (BSh according to the Köppen-Geiger classification; Peel et al., 2007). At the eastern end of the Mediterranean Basin, the climate of the Khabur drainage exhibits hot dry summers and cool wet winters. The average temperature is $>30^{\circ}\text{C}$ during the summer and $<10^{\circ}\text{C}$ during the winter. Most of the cold-season precipitation is a result of mid-latitude troughs that propagate from the North Atlantic Ocean and reactivate over the Eastern Mediterranean Sea (Lionello et al., 2006). The Khabur Plains are characterized by a steep rainfall gradient and high inter-annual climate variability. There is strong annual fluctuation in precipitation, with no rain at all during the summer and quite abundant rains (40–60 mm on average per month) from December to April (climate-data.org). In the area of Hassake (Fig. 1), located 313 m above sea level, the mean annual precipitation (MAP) and temperature are about 290 mm/y^{-1} and 18°C , respectively (Weiss, 1986). The rainy season extends from December to April (80% of MAP), whereas rainfall in June, July, and August accounts for only 0.2% of the annual total.

Dry farming is possible in the areas with average annual precipitation $>300\text{ mm}$, but there is high inter-annual variability in rain abundance that makes farming risky.

In such climatic conditions, taking into account lower access to fresh water and higher evaporation rate during the summer, higher $\delta^{18}\text{O}$ values are expected for the dry and hot season. The main water sources for the region, apart from rainfall, are the Khabur and its permanent or temporal tributaries as the Wadi Jaghjagh and the Wadi Radd at a distance of $\sim 3.5\text{ km}$ from Tell Majnuna; some reliance of underground waters is also possible, although there is limited evidence of archaeological boreholes in the region.

MATERIAL

In the years 2006–2008, the British-Syrian archaeological expedition to Tell Brak, directed by Joan Oates and Augusta McMahon (Cambridge University), explored several mass burials at the mound of Tell Majnuna, located a few hundred metres north-west of Tell Brak and $\sim 30\text{ km}$ north-east of Hassake (Fig. 1). There were at least two large and a few smaller clusters of human bones belonging to individuals mainly between ~ 15 and 45 years of age (Sołtysiak, 2010).

Two teeth for the present analysis were selected from a small cluster labelled as EM loc. 25. It may be dated to the mid-4th millennium BCE, i.e. Late Chalcolithic 3/4. Radiocarbon dating of earlier and later strata is available, and therefore the date for EM loc. 25 may be estimated as between 3763–3519 calBC and 3519–3343 calBC. This bone assemblage reflects one of episodes of increased mortality that may have been the consequence of overpopulation and social conflicts at the site in the period of rapid urban growth (Sołtysiak, 2010; McMahon et al., 2011). The cluster EM loc. 25 contained remains of at least 8 individuals, mainly crania; the indi-

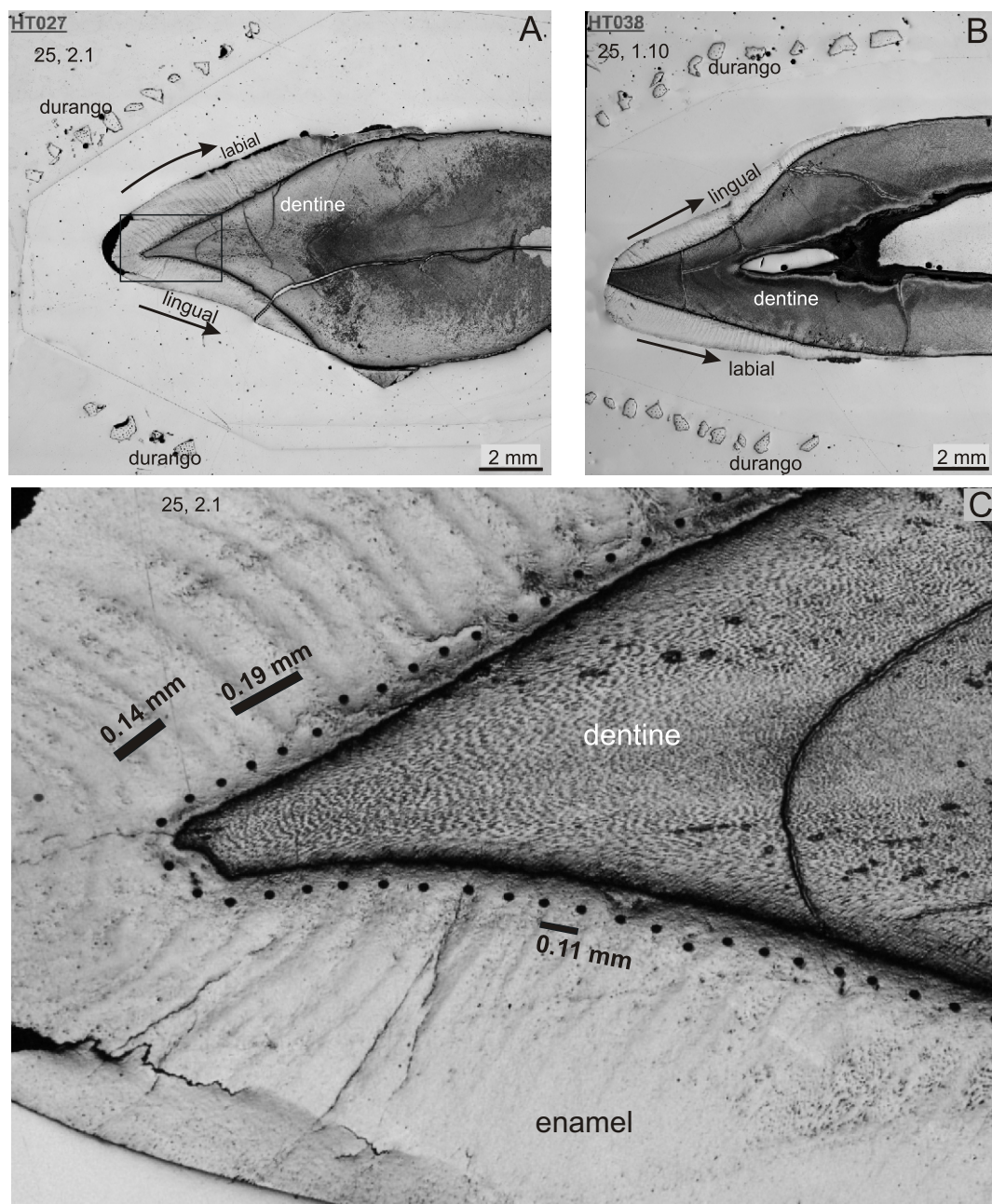


Fig. 3. Polished section of tooth samples imaged in reflected light of conventional microscope – showing a sample versus reference material layout in epoxy resin, tooth morphology and state of enamel preservation; note two steps of resin embedding

A – sample EM loc. 25, 2.1; **B** – sample EM loc. 25, 1.10; tracks of spots after oxygen isotope profiles are visible; **C** – top part of EM loc. 25, 2; crown – with histologically identified enamel structure striae of Retzius; thickness of successive layers varies from 0.06 to 0.20 mm; the innermost enamel layer of the incisal part of lingual side reveals a low degree of preservation; images are a composite stitched together from smaller pictures

Table 1

Factors affecting $\delta^{18}\text{O}$ values in surface waters (summary after Róžański et al., 1993; Gregoricka, 2011)

Correlation	Factors
Positive	water evaporation; air temperature; aridity
Negative	latitude; altitude; distance from the coast; precipitation

vidual 2.1 was likely a young female, and the individual 1.10 was an adolescent with no sex determination. Their upper canines were selected for the analysis, as their enamel is thicker than on other teeth, and this makes the measurements easier. On average, the enamel of permanent upper canines starts developing at the age of 9 months and the crown is complete by the age of 5.5 years (Reid and Dean, 2000), although the process of maturation can continue later. Therefore, if enamel is complete, it should be theoretically possible to observe four or five peaks of $\delta^{18}\text{O}$ value reflecting hot and dry summer.

ANALYTICAL PROCEDURE

Analytical works were performed at the Ion Microprobe Section of the Polish Geological Institute – National Research Institute in Warsaw using *SHRIMP IIe/MC* instrument. All samples for SIMS technique, including ancient biological material, must be solid and high-vacuum resistant (Ireland et al., 2008; Ickert et al., 2008; Kita et al., 2009). Moreover, the target surface must be flat, with exposed object of interest, and electrically conductive.

Due to the frequent presence of large cracks within teeth from archaeological sites, initial epoxy impregnation was required before mount preparation. Human teeth were embedded in epoxy resin to stabilize all components, and then precisely sectioned in the labial-lingual plane to expose the largest possible part of enamel. Only a half of teeth were chosen for analysis. SIMS method requires repeated calibration using reference materials with a chemical composition similar to that of the analysed target samples. Therefore, sample preparation and analytical works are concerned on an enamel bioapatite sample and apatite reference material.

Natural apatite from the Cerro de Mercado Fe-mine, Durango, Mexico (Frei et al., 2005), so-called “Durango” ($\delta^{18}\text{O}_{\text{apatite}} = 9.8\text{‰}$), has been used to calibrate SIMS $\delta^{18}\text{O}$ measurements on human teeth. Although not perfectly homogeneous (e.g., Boyce and Hervig, 2005; Sun et al., 2015), Durango apatite is routinely used as a standard reference material (e.g., Aubert et al., 2012).

A tooth and reference apatite were placed within 5 mm of the centre of the mount (Ickert et al., 2008; Kita et al., 2009) to minimize instrumental bias associated with sample position. The sectioned tooth, including enamel, was positioned upon a double-sided tape together with Durango grains, and attached by epoxy resin (Struers Epofix). For biological samples, Araldite resin could be also accepted if backscattered electron BSE or cathodoluminescence electron microprobe CL imaging is not necessary. The best results are obtained when the samples are produced as “Megamounts” of 35 mm diameter (Ickert et al., 2008).

Hardened mounts were polished using 1200 grade SiC paper and 1 μm diamond paste. Prior to analysis, the mounts were cleaned in high-purity ethanol using an ultrasonic bath and dried during a few days in a vacuum heater. No chemicals or chemical reactions were used for sample preparation. Each mount was coated with a 15 nm high-purity gold layer to assure an electric conductivity. Mount should enter the vacuum system in advance of the analytical session. A basic instrumental configuration and analytical procedures were similar to those detailed by Ickert et al. (2008) and Aubert et al. (2012). The *SHRIMP IIe/MC* in PGI was operated in a multi-collector, negative ion mode. A 15 kV, 10 nA Cs^+ primary ion beam was focused to a 20 μm diameter spot on the Au-coated target, producing 250–300 pA of secondary ^{16}O . The mounts with human tooth were analysed during two independent sessions in November 2015 (28th and 30th) using automatic run, lasting about 23 hours and 28 hours, respectively. Two masses ^{16}O and ^{18}O were measured simultaneously on Faraday cups with a resolution of about 1800R. Target charging was neutralized using 330 eV electrons from an oblique-incidence focused electron gun. Prior to analysis, the target area on the sample was pre-sputtered for 90 s using a 20 μm diameter area raster, thereby locally removing the gold coat and implanting an initial Cs dose prior to the onset of data acquisition. The *SHRIMP* instrument was operated with a mass resolution $R (M/\Delta M) \sim 1800$, which is sufficient to resolve mass ^{18}O versus ^{16}O , H_2 isobaric interfer-

ences existed within the bioapatitic target composition. Enamel was sampled by a single spot of 0.02 mm in size at $\sim 0.12\text{--}0.15$ mm intervals (Fig. 2).

Oxygen isotope ratios are reported related to the Vienna Standard Mean Ocean Water (VSMOW) and expressed as parts per mil. Analyses were corrected for a small amount of isotopically fractionated electron-induced secondary ion emission EISE (Ickert et al., 2008). The data were processed using *POXI* internal *SHRIMP* user software that took account of any long-term drift in baselines and/or isotopic fractionation.

Before and after ion microprobe analysis, sample imaging was prepared using a reflected light RL of optical microscope. The dimensions of the enamel layer were determined by measuring the distance along the connection between dentine (dark) and enamel using *NIS Elements BR* software on a *Nikon Eclipse LV100N Pol* optical microscope (Fig. 3). After the analytical session, a *HITACHI SU3500* Scanning Electron Microscope (SEM) was used to document the proper spot locations within the innermost enamel layer by low-magnification SEM and backscattered electron (BSE) images.

AUTHENTICATION

There are many factors that may produce error in observed biogenic $\delta^{18}\text{O}$ values, as diagenetic processes, sample contamination at the preparation stage, instrumental drift or distortion. To assure that real biogenic signal is detected, two different authentication protocols were applied:

- measurement control with use of the Durango reference material;
- comparison between labial and lingual side.

The $\delta^{18}\text{O}$ value of Durango reference apatite relative to VSMOW was taken as 9.82‰ (comparable with Durango 3) composition of $9.81 \pm 0.25\text{‰}$ measured by Lécuyer et al. (1998) and $9.80 \pm 0.25\text{‰}$, independently determined by C. Lécuyer using the GIRMS method (Rigo et al., 2012). Durango was analysed first, then again after every three spots of studied samples. Carefully chosen, transparent and inclusion-free chips of gem quality Durango usually yield proper internal consistency of $\delta^{18}\text{O}$ with standard deviation (s.d.) ~ 0.3 calculated from $n = 30$ to 40 analyses of each session, and precision of each determination $< 0.2\text{‰}$, that has to be always controlled.

In every tooth, two lines of measurements were designed, one on the labial and one on the lingual side. It is possible to identify spots on both sides that correspond to roughly the same formation time and – if we deal with biogenic signal – their expected $\delta^{18}\text{O}$ values should differ no more than the instrumental measurement error. We calculate the difference between means and distributions of $\delta^{18}\text{O}$ values on the labial and lingual sides. In this paper, as no counting of enamel layers was available, low difference between mean values and lack of significance of the Kruskal-Wallis test between the labial and lingual sides of the same tooth compared to significant differences between different teeth were taken as the evidence of mainly biogenic origin of observed pattern.

RESULTS

The thickness of tooth enamel exposed by the section gradually increases to the maximum of 1.38–1.40 mm, and the preserved length of enamel varies between 6.66 and 11.57 mm (Table 2). The dimensions of the enamel layer between the labial and lingual sides and between individuals are variable. Typ-

Table 2

Basic parameters of studied enamel layers of human teeth from Tel Majnuna, and taken measurements

Sample ID	Max width [mm]	Length mm]	Profile length [mm]	Number of spots [n]	Average distance between spots [mm]	Profile record [%]
EM loc. 25, 2.1 labial (A) (HT27)	1.38	9.93	9.86	85	0.116	99.29
EM loc. 25, 2.1 lingual (B) (HT27)	1.22	6.66	6.46	58	0.111	96.99
EM loc. 25, 1.10 labial (A) (HT38)	1.40	11.95	11.70	79	0.148	97.91
EM loc. 25, 1.10 lingual (B) (HT38)	1.18	11.57	11.50	98	0.116	99.39

ically, the analysis covered >95% of exposed length of enamel, omitting cracked or damaged parts. The inner layer was identified visually as a thin aprismatic layer adjacent to the enamel-dentine junction EDJ (Figs. 2 and 3).

The single spots were placed within the inner matured enamel layer along EDJ according to incremental chronology along the axis of growth, from the incisal (older) to apical (newer) enamel. The distance between neighboring spots varies from 0.10 to 0.12 mm, being matched to the thickness of each incremental layer of both sides (Fig. 3C). Longer and various distances (tooth 1.10) from 0.12 to 0.15 mm were also tested.

The standard error of any one from 144 (EM 25, 2.1) and 177 (EM 25, 1.10) single spot enamel analysis was usually better than 0.2‰ ($1\delta \pm 0.05\text{--}0.2\text{‰}$), except initial 20 points on the labial side of sample 25, 2.1 along the zone of visible defects of enamel (Fig. 3C). The reference Durango apatite yielded a mean $\delta^{18}\text{O}$ value of $9.83 \pm 0.10\text{‰}$ (1σ) and of $9.82 \pm 0.05\text{‰}$ (1σ). The precision of each determination was usually 0.1–0.2‰. The standard deviation for repeated analyses of Durango for each session was 0.67 ($n = 58$) and 0.42‰ ($n = 66$). The isotopic $\delta^{18}\text{O}$ ratio along the enamel dentine junction varies from $16.22 \pm 0.09\text{‰}$ to $21.23 \pm 0.08\text{‰}$ in EM 25, 2.1, and from $15.58 \pm 0.10\text{‰}$ to $19.24 \pm 0.10\text{‰}$ in EM 25, 1.10 (Table 3).

The minimum and maximum values on both sides of tooth are not always identical and do not always correspond to the same distances from the apex. The mean average values for each side within one tooth are rather similar. Inconsistency between EM 25, 2.1 and EM 25, 1.10 does not exceed 1‰. Intra-tooth variation in the oxygen isotopic composition (up to

5‰) was observed in the enamel of individual EM 25, 2.1. A smaller amplitude of variations up to 3.5‰ was documented in the case of sample EM 25, 1.10. These minor fluctuations in sample 25, 1.10 are emphasized by lower standard deviation s.d. of 0.61–0.66 calculated for the mean $\delta^{18}\text{O}$ value.

The graphical form of stable oxygen isotope composition with standard errors is presented on the diagrams for each side and tooth separately (Figs. 4 and 5). To document a layout of analysed points and continuity of the profile, additional plots using SHRIMP instrumental coordinates of the sample stage position are also shown.

Lack of the initial part of enamel from the occlusal side of EM 25, 1.10 on both sides causes some problems with synchronization between the lingual vs labial record (Fig. 5). The sequential analyses form a profile line along the enamel-dentine junction. The non-uniform distance between spots applied to the labial and lingual sides resulted in differences in the profiles obtained from each side of enamel, but regular repeatability of $\delta^{18}\text{O}$ fluctuations is visible. Profiles for EM 25, 2.1 and EM 25, 1.10 reveal 4 and 3 peaks, respectively, with an almost similar pattern for both sides. The isotopic record is complete only for sample EM 25, 2.1 and the pattern of $\delta^{18}\text{O}$ profile of the labial side has an equivalent in the lingual side (Fig. 4). The zone on the top of the labial side, where micro-cracks are visible, yielded quality values of $\delta^{18}\text{O}$ with poorer internal precision (larger standard errors).

For authentication of the results, the non-parametric Kruskal-Wallis test has been applied. For all four datasets $H = 36.79$, and $p = 0.0000$. The pair-wise comparisons are shown in Table 4. It is clear that the variance between the teeth (bold val-

Table 3

Summary of oxygen $\delta^{18}\text{O}$ isotope results from two human teeth from Tell Majnuna

Sample ID	Number of spots	$\delta^{18}\text{O}$ max [‰]	s.e [‰]	$\delta^{18}\text{O}$ min. [‰]VSMOW	s.e [‰]	Range [‰]VSMOW	$\delta^{18}\text{O}$ Average [‰]VSMO	s.e [‰]	s.d
EM loc. 25, 2.1 labial (A) (HT27)	85	21.23	0.08	16.24	0.10	4.99	18.63	0.12	1.11
EM loc. 25, 2.1 lingual (B) (HT27)	58	20.38	0.07	16.22	0.09	4.16	18.55	0.3	1.97
EM loc. 25, 1.10 labial (A) (HT38)	79	19.02	0.10	16.52	0.06	2.51	17.84	0.06	0.61
EM loc. 25, 1.10 lingual (B) (HT38)	98	19.24	0.10	15.58	0.10	3.66	18.08	0.07	0.66

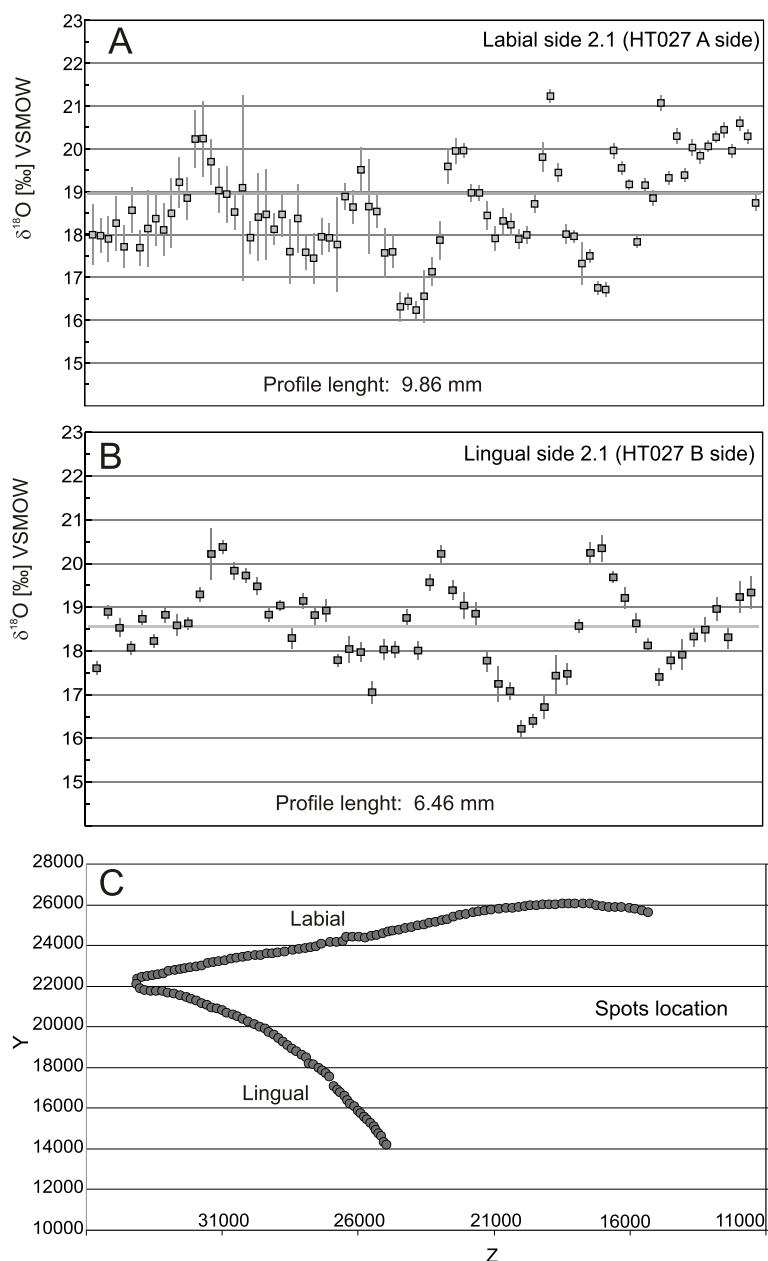


Fig. 4. The oxygen isotope composition from the innermost enamel layer of EM loc. 25, 2.1 tooth (HT027)

Single spot profile measured along: **A** – labial side, and **B** – lingual side; error bars are 2σ ; **C** – diagram on the sample-stage coordinates *Y* versus *Z* (number of steps), that document the positions of each single spot; note strong correlation between results with lower precision (error bars) and a lower degree of preservation on the top lingual part of enamel/dentine junction

ues of $p < 0.05$) are significantly higher than the variance between the lingual and labial sides on the same tooth. First tooth (25, 2.1) shows greater compatibility between the sides than the other (25, 1.10), which results from the fact that the second one is more heavily worn and the starting points were formed at different times.

The tooth EM 25, 10.1 has an irregular area of enamel loss on the top, thus the sequential profiles are not synchronous, with records starting not at the same moments of enamel formation. Moreover, non-uniform distances between spots have been applied in this study. On the lingual side, spots are lo-

cated every 0.116 mm, but on the labial side – every 0.148 mm. A longer step (distance) between spots leads to visual inconsistencies of the $\delta^{18}\text{O}$ pattern, caused by omitting some peaks or troughs, but the general seasonal fluctuations are still detectable. Therefore, it is recommended to apply a uniform distance as dense as possible.

DISCUSSION

The application of oxygen isotope analyses and their advantage for palaeoclimatic study was demonstrated more than thirty years ago (Longinelli, 1984; Luz et al., 1984; Luz and Kolodny, 1985), although most of early investigations were based on measurements made by IRMS technique with its specific procedure and limitations. The oxygen isotope data existing in literature mostly reflect an averaged composition of dental tissue presented as a mean value of $\delta^{18}\text{O}$. Among many examples, we can quote a case of oxygen isotope investigations of human tooth enamel sampled from Medieval Greenland between 1400 and 1700 A.D, which provided only an averaged value for a single tooth (Fricke and O’Neil, 1996). It was concluded that for time interval overlapping the Little Ice Age, decreasing $\delta^{18}\text{O}$ values from $18.1 \pm 0.86\text{‰}$ to $11.6 \pm 0.60\text{‰}$ VSMOW may express a rapid cooling in northern Europe during the well-known period of climate coolness. Similarly averaged values of $\delta^{18}\text{O}_{\text{phosphate}}$ for each individuals in the range of $23.8\text{--}26.0\text{‰}$ VSMOW form a record from individual teeth of Nilotic Nubian mummies dating from 350–550 to 500–1400 A.D. (White et al., 2004). Collected data were discussed in terms of relationship between climate, level of the Nil River and diet. The authors concluded that intra-tooth microsampling is necessary to determine the real variability, which “would allow a finer resolution of the effects of seasonality”.

Traditional microsampling by microdrilling of mammalian tooth enamel allowed preparing 3 to 10 microsamples (Wiedemann-Bidlack et al., 2008; Britton et al., 2009; Tian et al., 2013; Wright, 2013; Zazzo et al., 2012), that means an average distance between pits in the range of about 1.2–2.0 mm. In consequence, conventional microsampling of enamel provides an isotopic average of different incremental layers. The ion microprobe *in situ* method offers a spatial resolution range about 10 times better than conventional microsampling. The advantage of SIMS is also the shallow analytical pit, only 1.5–2 μm deep; hence SIMS is recognized as the most sensitive surface analysis technique.

Unaltered area (BSE image – Fig. 2), along to the enamel/dentine junction EDJ selected for ion microprobe tests, retains an unchanged biogenic oxygen isotope signal that closely follows the chronology of incremental layers of permanent upper canines, that starts developing in the age of ~ 9 months, and completes by the age of 5.5 years (covering about 57–60 months).

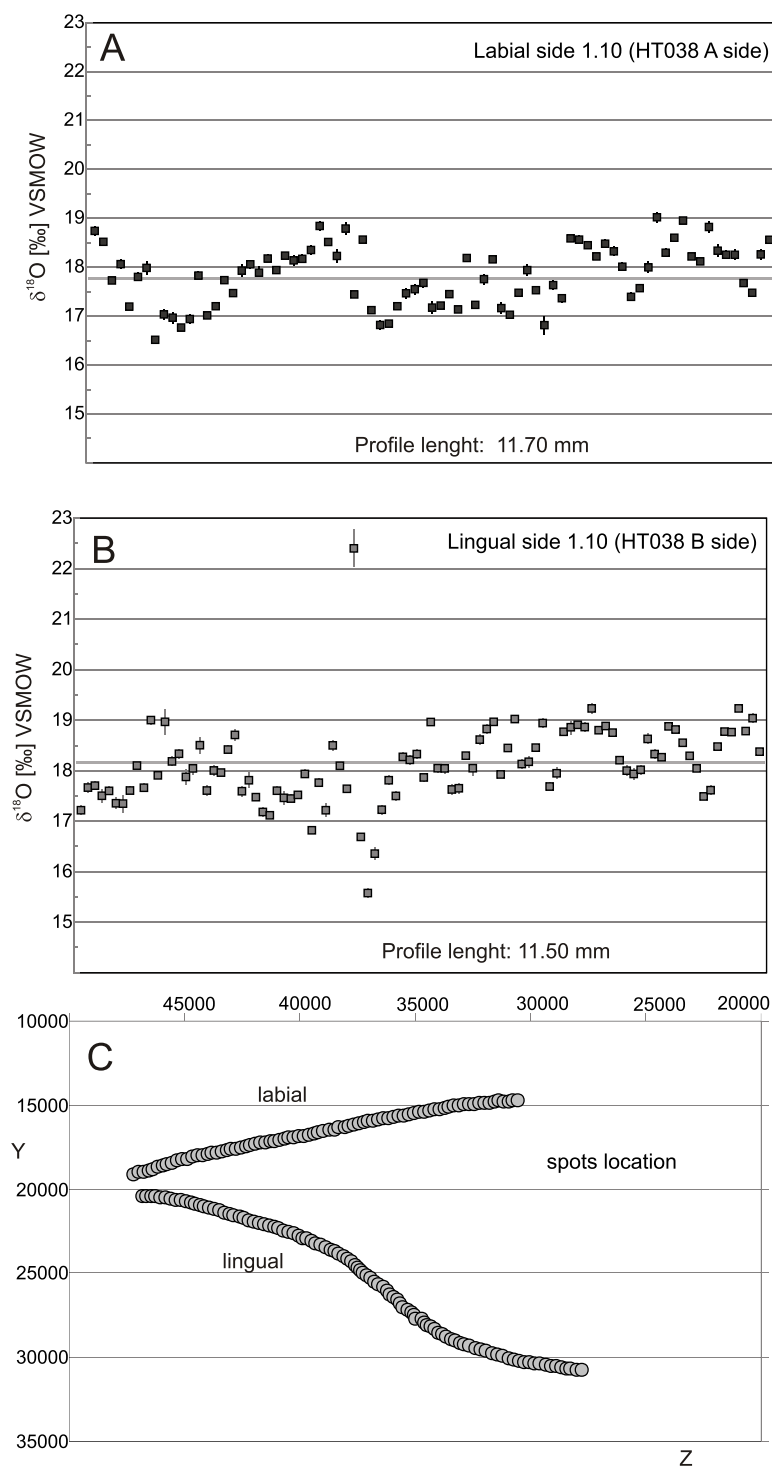


Fig. 5. The oxygen isotope composition from the innermost enamel layer of EM loc. 25, 1.10. tooth (HT038)

Single spot profile measured along: **A** – labial side, and **B** – lingual side; error bars are 2σ ; **C** – sample-stage coordinates *Y* versus *Z*, that document the positions of each single spot measurement

As an effect of *SHRIMP Ile/MC* ion microprobe analyses, ~60 to 100 $\delta^{18}\text{O}$ values from single spots located every 0.12–0.14 mm can be obtained from each side of human tooth, from incisal to apical ends, according to chronology of enamel mineralisation, that is enough to obtain temporal resolution of less than one month. The routine of two-side investigation in

case of human tooth analysis can also complete isotopic dataset if enamel is not fully preserved or if contains any defects (Figs. 3 and 4). In case of sample EM 25, 2.1, a lingual sequential profile improves the record of the defected labial side, but in case sample EM 25, 10.1, a lingual profile slightly completes the record of labial apex.

The average $\delta^{18}\text{O}$ values for two enamel samples, representing two individuals, differ only by 1‰. The variability a range of ~2–2.4‰ was reported for humans from one archeological sites as an example of variation of stationary population (White et al., 2004 and references therein).

There is no doubt that the oxygen enamel composition is a complex function of physiology, climate and diet. In consequence, a high spatial resolution $\delta^{18}\text{O}$ multi-year record is influenced by various factors (Table 1), but climatic parameters, such as local temperature and moisture availability, seem to be dominated and widely used for palaeoclimate reconstructions. There is one exception: if $\delta^{18}\text{O}$ analyses are performed on mammalian teeth affected by bacterial or microbial alteration the reconstruction could be invalid (Zazzo et al., 2004).

In case of human teeth from Tel Majnuna the single spot $\delta^{18}\text{O}$ results from the mostly unaltered inner layer along EDJ form an approximately sinusoidal pattern (Figs. 4 and 5), and the locations of major peaks and troughs coincide for each side (Fig. 6A, B). Such regular $\delta^{18}\text{O}$ variations reflect regular recurring fluctuations of oxygen composition of ingested water. It likely corresponds to seasonal fluctuations of meteoric water, with a higher ratio of heavy oxygen (^{18}O) to light oxygen (^{16}O) formed in response warm seasons, and a lower $\delta^{18}\text{O}$ ratio during cold and humid seasons. The $\delta^{18}\text{O}$ values of meteoric water (and river, lake, or groundwater with rainfall water inputs) in most continental locations are higher in summer and lower in winter. The $\delta^{18}\text{O}$ of enamel bioapatite and humidity or rainwater correlate negatively because $\delta^{18}\text{O}$ values of surface waters increase in dry settings (Kohn et al., 2002). A positive correlation is documented between $\delta^{18}\text{O}$ and temperature. There is no doubt that variations in the oxygen isotope composition of meteoric water are caused by seasonal climatic parameters, e.g. warm/cold months at high and mid latitudes (e.g., Różanski et al., 1993; Gregoricka, 2011). The altitude effect is weaker. Kattan (1997) found an oxygen $\delta^{18}\text{O}$ altitude effect of -0.23‰ per 100 m.

For an archaeological site at defined latitude and altitude (Tell Brak: $36^{\circ}44'42''\text{N}$, $41^{\circ}03'30''\text{E}$), considered as a “local” to the place of human teeth recovering, the annual climate graph for the nearest city of Hassake (<http://www.hassakah.climatemps.com/>) has been shown to illustrate maximal, minimal temperatures and precipitation values (Fig. 6C). Hassake is located in the continental part of Syria close to Tell Brak in the Khabur River drainage with the similar long distance from the coastline and the same features of semi-arid steppe climate. In the northeastern part of Syria, a hot season (summer) is from May to September. Most rainfall is seen in January, and most dry periods are in June, July and August (<http://weather-and-climate.com>). In

Table 4

Kruskal-Wallis test results, pair-wise comparisons: z' – values above the diagonal and p – values below the diagonal; $p < 0.05$ marked in bold

	25, 2.1 labial	25, 2.1 lingual	25, 1.10 labial	25, 1.10 lingual
25, 2.1 labial		0.01	5.27	3.20
25, 2.1 lingual	1.000000		4.77	2.87
25, 1.10 labial	0.000001	0.000011		2.31
25, 1.10 lingual	0.008387	0.024517	0.124847	

such climatic conditions, taking into account the lower access to fresh water and the higher evaporation rate during the summer, higher $\delta^{18}\text{O}$ values are very typical for the dry and warm season (Fig. 6A, B), that is confirmed by several environmental studies of atmospheric precipitation in Syria during 1989/1990 (Kattan, 1997) and currently (Zakhem and Hafes, 2010). From these data between successive troughs we can readily estimate the yearly range of isotope compositions. The maximum amplitude of $\delta^{18}\text{O}$ ~ 4 – 5‰ for one cycle season deciphered from the 2.1 pattern clearly corresponds to the strong annual fluctuation in precipitation, with quite abundant rains of 40–60 mm in average per month from January to April, and no rain at all during June–August summer (climate-data.org). The annual compilation of modern temperature and precipitation values and oxygen $\delta^{18}\text{O}$ frequency presents a pattern of typical variation (Fig. 6C). The graph from the continental area of Tell Majnuna points to a high gradient of two basic climatic parameters and their seasonal fluctuations.

Environmental monitoring of the atmospheric precipitation in Syria during 1989/1990 and 1991/1993 (Kattan, 1997; Zakhem and Hafes, 2010) confirmed that a higher seasonal temperature and stable isotopes variations are observed at continental stations in comparison to coastal stations. Furthermore, the relation between monthly average $\delta^{18}\text{O}$ values and the monthly amount of precipitation in Syria shows high fluctuations at low rainfall values. The oxygen $\delta^{18}\text{O}$ frequency distribution in the continental area manifests two peaks: the higher one during the rainy season in winter is at about -8‰ (January), and the lower one during the lower rainfall is at -2‰ (August) (Zakhem and Hafes, 2010), that defines seasonal fluctuations in the range of $\pm 6\text{‰}$ or more www.waterisotopes.org (Fig. 6C).

Past inhabitants (4th millennium BCE) of this geographic region probably experienced a similar style of seasonality, but with various amplitudes of fluctuation from 4 to 5‰ (Fig. 6), which is comparable to the present-day amplitude of 6‰ (Zakhem and Hafes, 2010). Moreover, the long-term (1919–2008) variations of precipitation in Syria show high irregularity that allows for recognition of the climate anomalies, e.g. some trends towards drought between a regular pattern (Zakhem and Hafes, 2010). Irregular record of $\delta^{18}\text{O}$ variation in time for 3–4 seasons is presented on Figure 6 (locally weighted scatter plot smoothing, LOWESS). According to the rainfall amounts calculated from the oxygen isotopic record of Soreq cave speleotherms (Israel), several rapid and short-lived rainfall depletion periods have been recognized (Kuzucuoğlu, 2007 and references therein) in ancient Middle East between 5300 and 2150 BC. It is known as the Late Holocene climate deterioration period of irregularity (after the Mid-Holocene climatic optimum) expressed by an extremely variable but lower rainfall amount, de-

creasing precipitation, and temperature increasing from 4000 to 3000 BC.

The interpretation of data on climate monitoring needs much more complementary, integrated information. Histological technique has listed also other factors, such as stress or illness that can produce disruptions in enamel development (DiGangi and Moore, 2013). Moreover, enamel formation consists of multiple discontinuous stages of mineralisation, thus the record is rather damped relative to the variation in isotopic composition (Passey and Cerling, 2002). The results obtained from tooth 10.1 underline such difficultness in interpretation of the $\delta^{18}\text{O}$ human enamel record due to complexity of cultural behaviour. It is necessary to consider a more complex dietary that can provide an additional variable

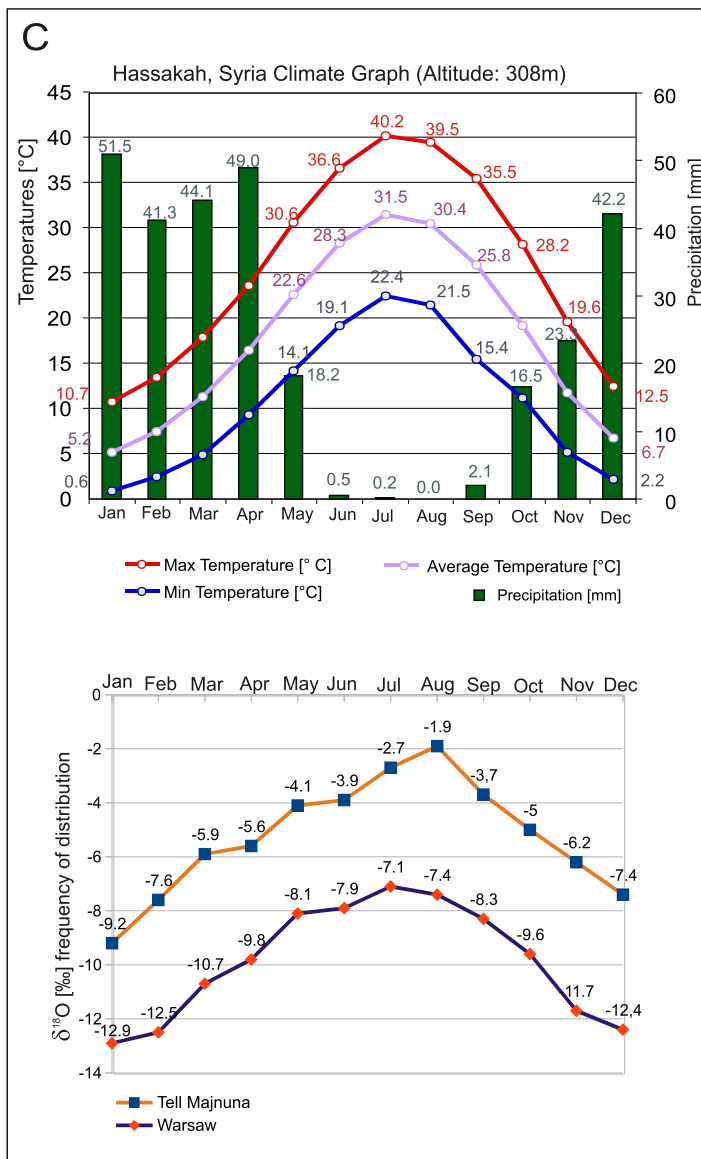
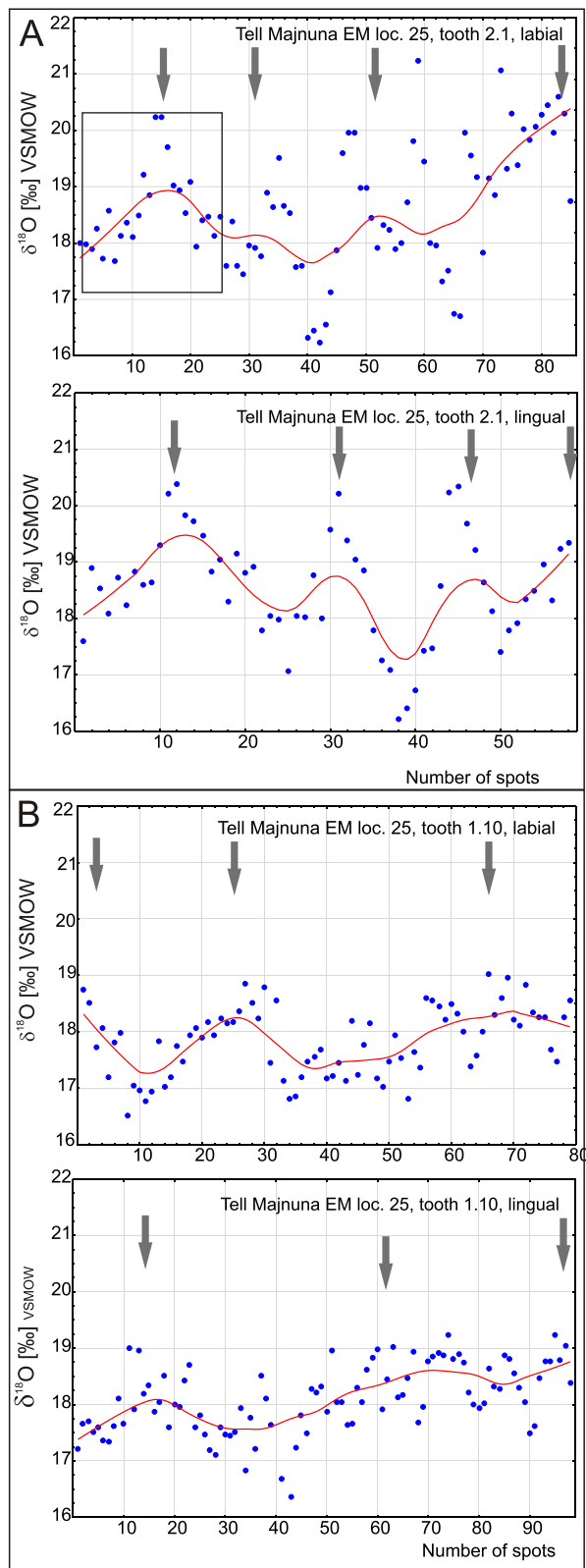
versus constant factors into the isotopic results, e.g. the problem of $\delta^{18}\text{O}$ preformed water and metabolic oxygen in food (Bryant and Froelich, 1996), or mixed surface water collects, which dampen the isotopic variation (Kohn and Cerling, 2002; Balasse, 2003). The human enamel does not perfectly follow the “time-line” of bioapatite mineralisation. The overall effect is probably blurred by some inertia in the enamel maturation.

However, the pattern of $\delta^{18}\text{O}$ detected in EM 25, 2.1 and 10.1 teeth from Tell Majnuna is roughly consistent with defined seasonal fluctuations expected in the area of semi-arid steppe climate in northeastern Syria (Hassaka), where strong annual fluctuations in precipitation are typical (Bowen et al., 2005; Bowen, 2015), but additional irregularities of the pattern have also been recognized. It demonstrates a validity of SIMS methodology of oxygen data collection. There is >12 spots between every peak or trough (Fig. 6A, B), which is enough to obtain a temporal resolution of less than one month. Oxygen isotopes in human inner dental enamel provides a short-term qualitative record of ancient climate deviations, but the statistical confirmation by testing a larger number of individuals from one archeological site is necessary. A sequential pattern of $\delta^{18}\text{O}$ provides a baseline that is useful for future comparison without the need to undertake complex conversions of the data from enamel to water $\delta^{18}\text{O}$ values, a process known to be problematic. Moreover, the seasonal fluctuation in $\delta^{18}\text{O}$ from human enamel may also potentially lead to the identification of local individuals vs. migrants or migration episode, which opens new avenues for investigation of archaeological material (e.g., Pellegrini et al., 2016).

CONCLUSIONS

This study has shown that $^{18}\text{O}/^{16}\text{O}$ isotope composition of human enamel can be determined in situ by SHRIMP *Ile*/MC ion microprobe with spatial resolution that is unobtainable by conventional microsampling methods. We established an effective analytical protocol for sequential analysing of $\delta^{18}\text{O}$ directly within the well-preserved inner enamel layer, along the enamel-dentine junction zone, that form a chronological pattern of $\delta^{18}\text{O}$ fluctuation for time of mineralization covering about 3–4 years.

We achieved an external precision of bioapatite $\delta^{18}\text{O}$ analysis below 0.2‰ [$\delta^{18}\text{O} \pm 0.15\text{‰}$ (1σ)]. *In situ* $\delta^{18}\text{O}$ profiling of an enamel layer is executed sequentially with high spatial resolution defined by 0.11–0.12 mm of the maximum distance between each spots and the analysed area not exceeding 0.02 mm in diameter, that correspond to temporal resolution less than a month. The best results are obtained using an undamaged inner thin enamel zone along the dentine junction according to geome-



6. Diagrams of $\delta^{18}\text{O}$ variation in time (using LOWESS), showing cyclical but irregular nature of isotopic fluctuation

A – the $\delta^{18}\text{O}$ pattern reflects the record of four seasonal (EM 25, 2.1); **B** – the $\delta^{18}\text{O}$ pattern reflects three seasonal cycles (EM 25, 1.10); the scale bar of vertical axis is fitted, but X-axis reflects only the number of spots; the maxima on both sides of the tooth are indicated with an arrow and one annual record is marked by square; **C** – graph showing an average monthly temperatures and precipitation in the area of NE Syria; <http://www.hassakah.climateemps.com/> and <http://weather-and-climate.com> and the oxygen $\delta^{18}\text{O}$ frequency distribution graph showing averaged monthly values for Tell Majnuna and Warsaw (data: www.waterisotopes.org)

try of maturation, with application of a two-side analytical procedure for preparing a labial versus lingual profile. Obtaining at least 60–100 precise $\delta^{18}\text{O}$ measurements on each side, holds particular promise for efforts directed at reconstructing seasonal shifts in humidity and temperature and other anomalies. A pattern of $\delta^{18}\text{O}$ isotopic profile corresponds to the conditions of relatively arid Middle East climate, with high seasonal differences in

rainfall and temperature on a multi-year scale, and documents a natural seasonality of the semi-arid steppe climate.

Therefore, the oxygen isotope composition collected from human teeth of two individuals from Tell Majnuna, a 4th millennium BCE cemetery in Northern Mesopotamia, have implications for methodology as well as for interpretation of $\delta^{18}\text{O}$ intra-tooth variation. These teeth recorded the environmental

input over a multi-year period of 4–5 years, thus represent important proxies for reconstructing environmental variation in $\delta^{18}\text{O}$ across different seasons of the few years with a resolution of less than one month.

Acknowledgements. The research on teeth from Tell Majnuna was financed by the National Science Centre (NCN) in Poland, grant No. 2013/10/M/HS3/00554. The preparation of analytical protocol for stable isotope sequential analyses

was supported by the Polish Geological Institute – National Research Institute internal grant no. 61.3207.1502.00.0 in 2015. The authors would like to thank two anonymous Reviewers for their valuable comments and suggestions to improve the manuscript. Moreover, gratefully acknowledged is the technical advice provided by A. Bebel (UW) and M. Rechowicz (PGI-NRI) during the mounts preparation procedure that required several tests and innovations.

REFERENCES

- Amiot, R., Lécuyer, C., Buffetaut, E., Escarguel, G., Fluteau, F., Martinneau, F., 2006. Oxygen isotopes from biogenic apatites suggest widespread endothermy in Cretaceous dinosaurs. *Earth and Planetary Science Letters*, **246**: 41–54.
- Aubert, M., Williams, I.S., Boljkovac, K., Moffat, I., Moncel, M.-H., Dufour, E., Grün, R., 2012. *In situ* oxygen isotope micro-analysis of faunal material and human teeth using a SHRIMP II: a new tool for palaeo-ecology and archaeology. *Journal of Archaeological Science*, **39**: 3184–3194.
- Ayliffe, L.K., Chivas, A.R., Leakey, M.G., 1994. The retention of primary oxygen isotope composition of fossil elephant skeletal phosphate. *Geochimica et Cosmochimica Acta*, **58**: 5291–5298.
- Babu, C.A., Samah, A.A., Varikoden, H., 2011. Rainfall climatology over Middle East region and its variability. *International Journal of Water Resources and Arid Environments*, **1**: 180–192.
- Balasse, M., 2003. Potential biases in sampling design and interpretation of intra-tooth isotope analysis International. *Journal of Osteoarchaeology*, **13**: 3–10.
- Blaise, E., Balasse, M., 2011. Seasonality and season of birth of modern and late Neolithic sheep from south-eastern France using tooth enamel $\delta^{18}\text{O}$ analysis. *Journal of Archaeological Science*, **38**: 3085–3093.
- Blumenthal, S.A., Cerling, T.E., Chritz, K.L., Bromage, T.G., Kozdon, R., Valley, J.W., 2014. Stable isotope time-serie in mammalian teeth: *in situ* $\delta^{18}\text{O}$ from innermost enamel layer. *Geochimica et Cosmochimica Acta*, **124**: 223–236.
- Bowen, G.J., 2015. The Online Isotopes in Precipitation Calculator, version 2.2. <http://www.waterisotopes.org>
- Bowen, G.J., Wassenaar, L.I., Hobson, K.A., 2005. Global application of stable hydrogen and oxygen isotopes to wildlife forensics. *Oecologia*, **143**: 337–348.
- Boyce, J.W., Hervig, R.L., 2005. U and Th zoning in Cerro de Mercado (Durango, Mexico) fluorapatite: insights regarding the impact of recoil distribution of 4He on (U-Th)/He Thermochronology. *Chemical Geology*, **219**: 261–274.
- Britton, K., Grimes, V., Dau, J., Richards, M.P., 2009. Reconstructing faunal migration using intra-tooth sampling and strontium and oxygen isotope analyses a case study of modern caribou (*Rangifer tarandus granti*). *Journal of Archeological Science*, **36**: 1163–1172.
- Britton, K., Fuller, B.T., Tütken, T., Mays, S., Richards, M.P., 2015. Oxygen isotope analysis of human bone phosphate evidences weaning age in archaeological populations. *American Journal of Physical Anthropology*, **157**: 226–241.
- Bryant, J.D., Froelich, P.N., 1995. A model of oxygen isotope fractionation in body water of largemammals. *Geochimica Cosmochimica Acta*, **59**: 4523–4537.
- Bryant, J.D., Froelich, P.N., 1996. Oxygen isotope composition of human tooth enamel from medieval Greenland: linking climate and society: comment and reply. *Geology*, **24**: 477–478.
- DiGangi, E.A., Moore, M.K., 2013. *Research Methods in Human Skeletal Biology*. Elsevier.
- Dolphin, A., Teeter, M.A., White, Ch., Longstaffe, F.J., 2016. Limiting the impact of destructive analytical techniques through sequential microspatial sampling of the enamel from single teeth. *Journal of Archeological Science: reports*, **5**: 537–541.
- Dupras, T.L., Schwarcz, H.P., 2001. Strangers in a strange land: stable isotope evidence for human migration in the Dakhleh Oasis, Egypt. *Journal of Archaeological Sciences*, **28**: 1199–1208.
- Eanes, E.D., 1979. Enamel apatite: chemistry, structure and properties. *Journal of Dental Research*, **58**: 829–836.
- Enax, J., Prymek, O., Raabe, D., Epple, H., 2012. Structure, composition, and mechanical properties of shark teeth. *Journal of Structural Biology*, **178**: 290–299.
- Frei, D., Harlov, D., Dulski, P., Rønso, J., 2005. Apatite from Durango (Mexico) – a potential standard for *in situ* trace element analysis of phosphates. *Goldschmidt Conference Abstracts 2005 Analytical Geochemistry*: A79.
- Fricke, H.C., O'Neil, J.R., Lynnerup, N., 1995. Oxygen isotope composition of human tooth enamel from medieval Greenland: linking climate and society. *Geology*, **23**: 869–872.
- Fricke, H.C., O'Neil, J.R., 1996. Inter- and intra-tooth variation in the oxygen isotope composition of mammalian tooth enamel phosphate: implications for palaeoclimatological and palaeobiological research. *Palaeogeography, Palaeoclimatology, Palaeoecology*, **126**: 91–99.
- Fricke, H.C., Clyde, W.C., O'Neil, J.R., 1998. Intra-tooth variations in $\delta^{18}\text{O}$ (PO_4) of mammalian tooth enamel as a record of seasonal variations in continental climates. *Geochimica et Cosmochimica Acta*, **62**: 1839–1850.
- Gregoricka, L.A., 2011. Mobility, exchange and tomb membership in Bronze Age Arabia. *Biochemical Investigation*. Dissertation, the Ohio State University.
- Hillson, S., 1996. *Dental Anthropology*. Cambridge University Press, Cambridge.
- Iacumin, P., Bocherens, H., Mariotti, A., Longinelli, A., 1996. Oxygen isotope analyses of co-existing carbonate and phosphate in biogenic apatite: a way to monitor diagenetic alteration of bone phosphate? *Earth and Planetary Science Letters*, **142**: 1–6.
- Ickert, R.B., Hiess, J., Williams, I.S., Holden, P., Ireland, T.R., Lanc, P., Schram, N., Foster, J.J., Clement, S.W., 2008. Determining high precision, *in situ*, oxygen isotope ratios with a SHRIMP II: analyses of MPI-DING silicate-glass reference materials and zircon from contrasting granites. *Chemical Geology*, **257**: 114–128.
- Ireland, T.R.S., Clement, S.W., Compston, W., Foster, J.J., Holden, P., Jenkins, B., Lanc, P., Schram, N., Williams, I.S., 2008. Development of SHRIMP. *Australian Journal of Earth Sciences*, **55**: 937–954.
- Jay, M., 2009. Breastfeeding and weaning behaviour in archaeological populations: evidence from the isotopic analysis of skeletal materials. *Childhood in the Past*, **2**: 163–178.
- Kattan, Z., 1997. Chemical and environmental isotope study of precipitation in Syria. *Journal of Arid Environments*, **35**: 601–615.
- Kita, N.T., Ushikubo, T., Fu, B., Valley, J.W., 2009. High precision SIMS oxygen isotope analysis and the effect of sample topography. *Chemical Geology*, **264**: 43–57.

- Kohn, M.J., Cerling, T.E., 2002.** Stable isotope composition of biological apatite. *Reviews in Mineralogy and Geochemistry*, **48**: 455–488.
- Kohn, M.J., Schoeninger, M.J., Valley, J., 1998.** Variability in oxygen isotope composition of herbivore teeth: reflections of seasonality or developmental physiology. *Chemical Geology*, **152**: 97–112.
- Kohn, M.J., Miselis, J.L., Fremd, T.J., 2002.** Oxygen isotope evidence for progressive uplift of the Cascade Range, Oregon. *Earth and Planetary Science Letters*, **204**: 151–165.
- Krzemińska, E., Czupyt, Z.J., 2015.** The $\delta^{18}\text{O}$ record explored within a dental targets by SHRIMP IIe/MC. *Mineralogical Magazine – Goldschmidt 2015; Abstracts*: 1701.
- Kuzucuoğlu, C., 2007.** Climatic and Environmental trends during the third Millennium B.B. in Upper Mesopotamia. In: *Sociétés humaines et changement climatique à la fin du troisième millénaire: une crise a-t-elle eu lieu en Haute Mésopotamie?*, Actes du Colloque de Lyon (5–8 décembre 2005), édité par Catherine Kuzucuoğlu et Catherine Marro. Institut Français d'Études Anatolies Georges Dumezil, 2007: 459–480.
- Lécuyer, C., Grandjean, P., Barrat, J.-A., Nolvak, J., Emig, C., Paris, F., Robardet, M., 1998.** $\delta^{18}\text{O}$ and REE contents of phosphatic brachiopods: a comparison between modern and lower Paleozoic populations. *Geochimica et Cosmochimica Acta*, **62**: 2429–2436.
- Lee-Thorp, J.A., van der Merwe, N.J., 1991.** Aspects of the chemistry of modern and fossil biological apatites. *Journal of Archaeological Science*, **18**: 343–354.
- LeGeros, R.Z., Trautz, O.R., Klein, E., LeGeros, J.P., 1969.** Two types of carbonate substitution in the apatite structure. *Experimentia*: **25**: 5–7.
- Lightfoot, E.C., O'Connell, T.C., 2016.** On the use of biomineral oxygen isotope data to identify human migrants in the archaeological record: intra-sample variation, statistical methods and geographical considerations. Edited by Luca Bondioli. *PLOS ONE*, **11**: e0153850.
- Lionello, P., Malanotte-Rizzoli, P., Boscolo, R., 2006.** *Mediterranean Climate Variability*. Elsevier, Amsterdam.
- Longinelli, A., 1984.** Oxygen isotopes in mammal bone phosphate: a new tool for paleohydrological and paleoclimatological research? *Geochimica et Cosmochimica Acta*, **48**: 385–390.
- Luz, B., Kolodny, Y., 1985.** Oxygen isotope variations in phosphate of biogenic apatites, 4. Mammal teeth and bones. *Earth and Planetary Science Letters*, **75**: 29–36.
- Luz, B., Kolodny, Y., Horowitz, M., 1984.** Fractionation of oxygen isotopes between mammalian bone-phosphate and environmental drinking water. *Geochimica et Cosmochimica Acta*, **48**: 1689–1693.
- McMahon, A., Sołtysiak, A., Weber, J., 2011.** Late Chalcolithic mass graves at Tell Brak, Syria, and violent conflict during the growth of early city-states. *Journal of Field Archaeology*, **36**: 201–220.
- Nanci, A., 2013.** *Ten Cate's Oral Histology: Development, Structure, and Function*. Elsevier.
- O'Neil, J.R., Reinhard, R.E., Blake, E.R., 1994.** A rapid and precise method of oxygen isotope analysis of biogenic phosphate. *Israel Journal of Earth Science*, **43**: 203–212.
- Pan, Y., Fleet, M.E., 2002.** Compositions of the apatite-group minerals: substitution mechanisms and controlling factors. *Reviews in Mineralogy and Geochemistry*, **48**: 13–49.
- Passey, B.H., Cerling, T.E., 2002.** Tooth enamel mineralization in ungulates: implications for recovering a primary isotopic time-series. *Geochimica et Cosmochimica Acta*, **66**: 3225–3234.
- Peel, M. C., Finlayson, B. L., McMahon, T. A., 2007.** "Updated world map of the Köppen-Geiger climate classification". *Hydrology and Earth System Sciences*, **11**: 1633–1644.
- Pellegrini, M., Pouncett, J., Jay, M., Pearson, M.P., Michael, P., Richards, M.R., 2016.** Tooth enamel oxygen "isoscapes" show a high degree of human mobility in prehistoric Britain. *Scientific Reports*, **6**: 34986.
- Pflug, K.P., Schuster, K.-D., Pichotka, J.P., Forstel, H., 1979.** Fractionation effects of oxygen isotopes in mammals. In: *Stable Isotopes: Proceedings of the Third International Conference* (eds. E.R. Klein and P.D. Klein): 553–561. Academic Press, New York.
- Reid, D.J., Dean, M.C., 2000.** The timing of linear hypoplasias on human anterior teeth. *American Journal of Physical Anthropology*, **113**: 135–139.
- Rigo, M., Trotter, J.A., Preto, N., Williams, I.S., 2012.** Oxygen isotopic evidence for Late Triassic monsoonal upwelling in the north-western Tethys. *Geology*, **40**: 515–518.
- Robinson, C., Weatherell, J.A., Hallsworth, A.S., 1971.** Variation in composition of dental enamel within thin ground tooth sections. *Caries Research*, **5**: 44–57.
- Rózański, K., Araguas-Araguas, L., Gonfiantini, R., 1993.** Isotopic patterns in modern global precipitation. *American Geophysical Union Geophysical Monograph*, **78**: 1–36.
- Schoeninger, M.J., 1995.** Stable isotope studies in human evolution. *Evolutionary Anthropology*, **4**: 83–89.
- Shahack-Gross, R., Tchernov, E., Luz, B., 1999.** Oxygen isotopic composition of mammalian skeletal phosphate from the Natufian period, Hayonim cave, Israel: diagenesis and paleoclimate. *Geoarchaeology*, **14**: 1–13.
- Simmer, J.P., Fincham, A.G., 1995.** Molecular mechanisms of dental enamel formation. *Critical Reviews in Oral Biology and Medicine*, **6**: 84–108.
- Sønju Clasen, A.B., Ruyter, I.E., 1997.** Quantitative determination of type A and type B carbonate in human deciduous and permanent enamel by means of Fourier transform infrared spectrometry. *Advances in Dental Research*, **11**: 523–527.
- Sołtysiak, A., 2010.** *Death and Decay at the Dawn of the City. Interpretation of Human Bone Deposits at Tell Majnuna, Areas MTW, EM and EMS*. Instytut Archeologii, Warszawa.
- Sponheimer, M., Lee-Thorp, J.A., 1999.** Oxygen isotopes in enamel carbonate and their ecological significance. *Journal of Archaeological Science*, **26**: 723–728.
- Stevens, R.E., Balasse, M., O'Connell, T.C., 2011.** Intra-tooth oxygen isotope variation in a known population of red deer: implications for past climate and seasonality reconstructions. *Palaeogeography, Palaeoclimatology, Palaeoecology*, **301**: 64–74.
- Stuart-Williams, H.L.Q., Schwarcz, H.P., 1997.** Oxygen isotopic determination of climatic variation using phosphate from beaver bone, tooth enamel and dentine. *Geochimica et Cosmochimica Acta*, **61**: 2539–2550.
- Sun, Y., Joachimski, M., Wiedenbeck, M., 2015.** Gem-quality apatite as reference material for oxygen isotope analysis of biogenic apatite by the secondary ion mass spectrometry. *Mineralogical Magazine – Goldschmidt 2015, Abstracts*: 3033.
- Tafforeau, P., Bentaleb, I., Jaeger, J.-J., Martin, C., 2007.** Nature of laminations and mineralization in rhinoceros enamel using histology and X-ray synchrotron microtomography: potential implications for palaeoenvironmental isotopic studies. *Palaeogeography, Palaeoclimatology, Palaeoecology*, **246**: 206–227.
- Tian, X.S., Zhu, C., Shui, T., 2013.** Diets, eco-environments and seasonal variations recorded in mammalian tooth enamel from Shunshanji site, Sihony County, Jiangsu Province, China. *Chinese Science Bulletin*, **58**: 3788–3795.
- Tomczyk, J., Wierzbowski, H., Zalewska M., 2016.** Stable isotope record of human and sheep enamel carbonate from the Ancient Middle Euphrates Valley (Syria). *International Journal of Osteoarchaeology*, **26**: 599–609.
- Traylor, R.B., Kohn, M.J., 2017.** Tooth enamel maturation reequilibrates oxygen isotope compositions and supports simple sampling methods. *Geochimica et Cosmochimica Acta*, **198**: 32–47.
- Trotter, J.A., Williams, I.S., Barnes, C.R., Lécuyer, C., Nicoll, R.S., 2008.** Did cooling oceans trigger Ordovician biodiversification? Evidence from conodont thermometry. *Science*, **321**: 550–554.
- Trotter, J.A., Williams, I.S., Nicora, A., Mazza, M., Rigo, M., 2015.** Long-term cycles of Triassic climate change: a new $\delta^{18}\text{O}$ record from conodont apatite. *Earth and Planetary Science Letters*, **415**: 165–174.
- Tsutaya, T., Yoneda, M., 2015.** Reconstruction of breastfeeding and weaning practices using stable isotope and trace element analy-

- ses: a review. *American Journal of Physical Anthropology*, **156**: 2–21.
- Weiss, H., 1986.** The origins of Tel Leilan and the conquest of space in Third Millennium Mesopotamia In: *The Origins of Cities in Dry Farming Syria and Mesopotamia in the Third Millennium* (ed. B.C.H. Weiss): 71–108. Four Quarters Publishing Co., Guilford, Conn.
- Wheeley, J.R., Smith, M.P., Boomer, I., 2012.** Oxygen isotope variability in conodonts: implications for reconstructing Palaeozoic palaeoclimates and palaeoceanography. *Journal of the Geological Society*, **169**: 239–250.
- White, C., Longstaffe, F.J., Law, K.R., 2004.** Exploring the effects of environment, physiology and diet on oxygen isotope ratios in ancient Nubian bones and teeth. *Journal of Archaeological Science*, **31**: 233–250.
- White, C.D., Spence, M.W., Stuart-Williams, H.Q.L., Schwarcz, H.P., 1998.** Oxygen isotopes and the identification of geographical origins: the Valley of Oaxaca versus the Valley of Mexico. *Journal of Archaeological Science*, **25**: 643–655.
- Wiedemann-Bidlack, F.B., Colman, A.S., Fogel, M.L., 2008.** Phosphate oxygen isotope analysis on microsamples of biapatite: removal of organic contamination and minimization of sample size. *Rapid Communication Mass Spectrometry*, **22**: 1807–1816.
- Williams, I.S., Trotter, J.A., Rigo, M., Barnes, C.R., 2013.** Analysing conodont $\delta^{18}\text{O}$ by SIMS. *Mineralogical Magazine*, **77**: 2499.
- Wright, L.E., 2013.** Examining childhood diets at Kaminluyu, Guatemala, through stable isotopic analysis of sequential enamel microsamples. *Archaeometry*, **55**: 113–133.
- Zakheim, B.A., Hafez, R., 2010.** Climatic factors controlling chemical and isotopic characteristics of precipitation in Syria. *Hydrological Process*, **24**: 2641–2654.
- Zazzo, A., Lecuyer, C., Mariotti, A., 2004.** Experimentally-controlled carbon and oxygen isotope exchange between biapatites and water under inorganic and microbially-mediated conditions. *Geochimica et Cosmochimica Acta*, **68**: 1–12.
- Zazzo, A., Bendrey, R., Vella, D., Moloney, A.P., Monahan, F.J., Schmidt, O., 2012.** A refined sampling strategy for intra-tooth stable isotope analysis of mammalian enamel. *Geochimica et Cosmochimica Acta*, **84**: 1–13.
- Żarski, M., Winter, H., Nadachowski, A., Urbanowski, M., Socha, P., Kenig, K., Marcinkowski, B., Krzemińska, E., Stefaniak, K., Nowaczewska, W., Marciszak, A., 2017.** Stratigraphy and palaeoenvironment of Stajna Cave (southern Poland) with regard to habitation of the site by Neanderthals. *Geological Quarterly*, **61** (2): 350–369.